'94 KACC (1994. 10. 17 ~ 20)

Dynamic Hybrid Position/Force Control of 2 D.O.F. Flexible Manipulators

Tsuneo Yoshikawa Kensuke Harada

Department of Mechanical Engineering
Faculty of Engineering
Kyoto University
Yoshida Hon-machi, Sakyo-ku, Kyoto 606-01, Japan

Abstract

Dynamic hybrid position/force control of flexible manipulators is proposed. First, a 2 D.O.F. flexible manipulator is modeled using the spring-mass model. Second, the equation of motion considering the tip constraints is derived. Third, hybrid position/force control algorithm is derived. In this control algorithm, the differentiable order of the desired trajectory and the stability condition are different from the case of rigid manipulators. Lastly, to verify the effectiveness of the proposed control algorithm, simulation results are presented.

1 Introduction

In recent years, need for light-weight and high-mobility structures for industrial robots has developed. For use in space, long arms are needed that are light in comparison to their load. In such arms, their elasticity demands compensation of arm deformation and vibration.

Considering the task that these flexible manipulators have to perform, not only the end point position but also the force that the end point exerts to an object should be simultaneously controlled. Moreover, to control them fast and precisely, the arm dynamics should be considered in their control algorithm.

Many researches have been done on hybrid position/force control of rigid manipulators so far[1,2,3]. However, there are not so many researches controlling position and force of flexible manipulators. Matsuno and Yamamoto[4] proposed a dynamic hybrid control based on singular perturbation approach using the distributed parameters model. Spong[5] or ElMaraghy et al.[6,7] proposed a dynamic hybrid control of manipulators with flexible joints.

Several methods have proposed in dynamic trajectory tracking control of flexible manipulators[8,9,10,11]. These results can be extended to hybrid control. Hosoda and Yoshikawa modeled flexible links using a simple spring-mass model[12], and the trajectory tracking controller is constructed[11].

In this paper, a method for dynamic hybrid control of flexible manipulators is proposed. We model the flexible manipulator by using the spring-mass model. This model is simple enough to be suitable for the real-time control. First, the equation of motion is derived considering the force that the end point exerts on an object. Second, dynamic hybrid control algorithm is constructed. In this approach, the differentiable order of the desired trajectory is different from the case of rigid manipulators. There exists the zero-dynamics[10] in this system. The stability condition depends on this dynamics. Lastly, to verify the effectiveness of the proposed control algorithm, simulation results are presented.

2 Modeling

In this section, a 2 D.O.F. flexible manipulator is modeled. Fig.1 shows an overview of the manipulator used in this research. This flexible manipulator has two links which are driven by the motors in each joint. These links are very flexible. An end effector and a force sensor are attached at the tip of this manipulator. The weight of the links are considered to be light in comparison to that of the motors or the end effector. As shown in Fig.1, $\boldsymbol{r}_i (i = 1, 2)$ is the position vector of the tip of link i with respect to the inertial coordinate system Σ_0. $m_i (i = 1, 2)$ is the mass at the tip of link i. $l_i (i = 1, 2)$ is the length of link i. The deformation and the angular deformation of the tip of link i are denoted as δ_i and ϕ_i, respectively. $\theta_i (i = 1, 2)$ is the joint displacement of joint i.

We make a following assumptions to make a model of this arm:

1. Each flexible link is slender, homogeneous and can be regarded to be simple beams.

2. The mass of each link is light enough to be negligible in comparison to lumped mass at the tip of the link.

3. Friction of motors and joints are assumed to be negligible.

Under these assumptions, we use the spring-mass model shown in Fig.2, in which each flexible link is modeled by using a spring system and a rigid body attached at the tip of the mass-less link.

In this model, we add the following assumption to simplify:

4. The beam does not deform longitudinally.

Under these assumptions, the position vectors of link i are given by

$$\boldsymbol{r}_1 = l_1\boldsymbol{b}_1 + \delta_1\boldsymbol{a}_1, \tag{1}$$

$$\boldsymbol{r}_2 = \boldsymbol{r}_1 + l_2\boldsymbol{b}_2 + \delta_2\boldsymbol{a}_2, \tag{2}$$

where

$$\begin{aligned} \boldsymbol{a}_1 &= [-\sin\theta_1 \ \cos\theta_1]^T, \ \boldsymbol{b}_1 = [\cos\theta_1 \ \sin\theta_1]^T, \\ \boldsymbol{a}_2 &= [-\sin(\theta_1+\theta_2+\phi_1) \ \cos(\theta_1+\theta_2+\phi_1)]^T, \\ \boldsymbol{b}_2 &= [\cos(\theta_1+\theta_2+\phi_1) \ \sin(\theta_1+\theta_2+\phi_1)]^T. \end{aligned} \tag{3}$$

Adopting this model to the 2 D.O.F flexible manipulator, the relation between the force f_i, moment n_i, elastic displacement δ_i and angular elastic displacement ϕ_i is given by

$$\begin{bmatrix} f_i \\ n_i \end{bmatrix} = \begin{bmatrix} K_{ib} & K_{ie} \\ K_{ie}^T & K_{id} \end{bmatrix} \begin{bmatrix} \delta_i \\ \phi_i \end{bmatrix}, \tag{4}$$

where K_{ib}, K_{ie} and K_{id} are spring constants.

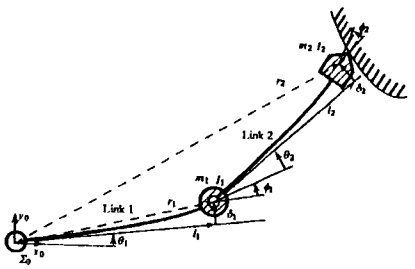

Fig.1 2 D.O.F. Flexible Manipulator

We derive the kinetic and potential energy of the manipulator. The total kinetic energy consists of that of lumped masses and rotational energy of motors such as

$$\begin{aligned} E_k &= \frac{1}{2}m_1\dot{\boldsymbol{r}}_1^T\dot{\boldsymbol{r}}_1 + \frac{1}{2}m_2\dot{\boldsymbol{r}}_2^T\dot{\boldsymbol{r}}_2 + \frac{1}{2}I_1(\dot\theta_1+\dot\phi_1)^2 \\ &\quad + \frac{1}{2}I_2(\dot\theta_1+\dot\theta_2+\dot\phi_1+\dot\phi_2)^2 + \frac{1}{2}I_{m1}(N_1\dot\theta_1)^2 \\ &\quad + \frac{1}{2}I_{m2}(\dot\theta_1+\dot\phi_1+N_2\dot\theta_2)^2, \end{aligned} \tag{5}$$

where $I_{mi}(i = 1, 2)$ is the rotational inertia of the ith motor, and $N_i(i = 1, 2)$ is the reduction ratio. $\dot{*}$ shows the differentiation with respect to time. The total potential energy is composed of that of elasticity in each link such as

$$\begin{aligned} E_p &= \frac{1}{2}\begin{bmatrix} \delta_1 \\ \phi_1 \end{bmatrix}^T \begin{bmatrix} K_{1b} & K_{1e} \\ K_{1e}^T & K_{1d} \end{bmatrix} \begin{bmatrix} \delta_1 \\ \phi_1 \end{bmatrix} \\ &\quad + \frac{1}{2}\begin{bmatrix} \delta_2 \\ \phi_2 \end{bmatrix}^T \begin{bmatrix} K_{2b} & K_{2c} \\ K_{2e}^T & K_{2d} \end{bmatrix} \begin{bmatrix} \delta_2 \\ \phi_2 \end{bmatrix}. \end{aligned} \tag{6}$$

Using the Lagrange's method, the equation of motion considering the force that the end point exerts on an object is derived as

$$\boldsymbol{M}(\boldsymbol{x})\ddot{\boldsymbol{x}} + \boldsymbol{h}(\boldsymbol{x}, \dot{\boldsymbol{x}}) + \boldsymbol{K}\boldsymbol{x} = \boldsymbol{D}\boldsymbol{\tau} - \boldsymbol{J}(\boldsymbol{x})^T\boldsymbol{F}, \tag{7}$$

where $\boldsymbol{x} = [\theta_1 \ \theta_2 \ \delta_1 \ \delta_2 \ \phi_1 \ \phi_2]^T$ is the vector of generalized coordinates, $\boldsymbol{\tau}$ is the vector of joint driving force, $\boldsymbol{M}(\boldsymbol{x})$ is the inertia matrix, $\boldsymbol{h}(\boldsymbol{x}, \dot{\boldsymbol{x}})$ is the vector of centrifugal and Coriolis force, $\boldsymbol{K}$ is the stiffness matrix, The matrix $\boldsymbol{D}$ has a 2×2 unity matrix in upper side and a 4×2 zero matrix in lower side, $\boldsymbol{J}(\boldsymbol{x})$ is the jacobian matrix of $\boldsymbol{x}$ with respect to $\boldsymbol{r}_2$, $\boldsymbol{F}$ is the 2 dimensional force vector that is exerted by the end effector. This equation of motion is simple and considered to be suitable for the real-time control.

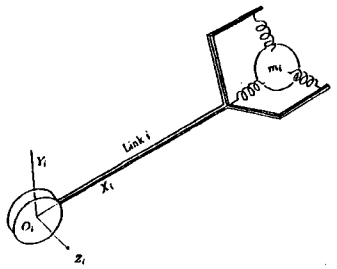

Fig.2 Spring-mass Model

3 Hybrid Position/Force Control

Using the equation of motion derived in the previous section, a hybrid position/force control algorithm is constructed in this section. Different from the case of rigid manipulators, it is not easy in flexible manipulators to obtain the joint displacements from the corresponding end point displacements and force (inverse kinematics problem), and to obtain the joint driving force (inverse dynamics problem). In the case of flexible manipulators, some special transformations are needed to construct a hybrid control algorithm.

First, we describe the kinematic equations. The end point position $\boldsymbol{r}_2$ is derived by using eq.(2). This equation is differentiated with respect to time as follows:

$$\dot{\boldsymbol{r}}_2 = \boldsymbol{J}(\boldsymbol{x})\dot{\boldsymbol{x}}, \tag{8}$$

$$\ddot{\boldsymbol{r}}_2 = \boldsymbol{J}(\boldsymbol{x})\ddot{\boldsymbol{x}} + \dot{\boldsymbol{J}}(\boldsymbol{x})\dot{\boldsymbol{x}}. \tag{9}$$

Arguments will be omitted in the following when no confusion occurs. The relation between the end point acceleration and the joint driving force is derived using eqs.(7)

and (9) as follows:

$$\ddot{\boldsymbol{r}}_2 = \boldsymbol{J}\boldsymbol{M}^{-1}\left(\boldsymbol{D}\boldsymbol{\tau} - \boldsymbol{J}^T\boldsymbol{F} - \boldsymbol{K}\boldsymbol{x} - \boldsymbol{h}\right) + \dot{\boldsymbol{J}}\dot{\boldsymbol{x}}. \quad (10)$$

In this equation, if $\boldsymbol{J}\boldsymbol{M}^{-1}\boldsymbol{D}$ is nonsingular, we can easily obtain a desired joint driving force from the desired end point acceleration and the desired force. However, as $\mathrm{rank}\boldsymbol{J}\boldsymbol{M}^{-1}\boldsymbol{D} = 1$ using the spring-mass model, we cannot directly obtain the joint driving force from eq.(10). So some approximations are used in eq.(10) as

5. Elastic displacements are small, so the terms which include δ_i or $\phi_i (i = 1, 2)$ are negligible except for the stiffness term.

6. Centrifugal and Coriolis force is small enough to be neglected.

Using the spring-mass model, the first term in the right-hand side of eq.(10), $\boldsymbol{J}\boldsymbol{M}^{-1}\boldsymbol{D}$, becomes a first order small term with respect to elastic displacements. Using these approximations, $\boldsymbol{J}\boldsymbol{M}^{-1}\boldsymbol{D}$ becomes 0. So eq.(10) is rewritten as follows:

$$\begin{aligned}\ddot{\boldsymbol{r}}_2 &\cong -\boldsymbol{J}\boldsymbol{M}^{-1}\left(\boldsymbol{J}^T\boldsymbol{F} + \boldsymbol{K}\boldsymbol{x}\right) \\ &\triangleq \boldsymbol{J}_F\boldsymbol{F} + \boldsymbol{J}_P\boldsymbol{x}. \end{aligned} \quad (11)$$

In eq.(11), there does not exist the term including the joint driving force $\boldsymbol{\tau}$. To get the desired joint driving force, the differentiation of eq.(11) is repeated and the eq.(7) is substituted until the coefficient of $\boldsymbol{\tau}$ becomes nonzero. Eq.(11) is differentiated with respect to time as

$$\begin{aligned}\boldsymbol{r}_2^{(3)} &= \boldsymbol{J}_P\dot{\boldsymbol{x}} + \dot{\boldsymbol{J}}_P\boldsymbol{x} + \boldsymbol{J}_F\dot{\boldsymbol{F}} + \dot{\boldsymbol{J}}_F\boldsymbol{F} \\ &\triangleq \tilde{\boldsymbol{J}}_P\dot{\boldsymbol{x}} + \boldsymbol{J}_F\dot{\boldsymbol{F}}. \end{aligned} \quad (12)$$

Eq.(12) is differentiated again as follows:

$$\boldsymbol{r}_2^{(4)} = \tilde{\boldsymbol{J}}_P\ddot{\boldsymbol{x}} + \boldsymbol{J}_F\ddot{\boldsymbol{F}} + \boldsymbol{v}_1, \quad (13)$$

where $\boldsymbol{v}_1$ is defined by

$$\boldsymbol{v}_1 = \dot{\tilde{\boldsymbol{J}}}_P\dot{\boldsymbol{x}} + \dot{\boldsymbol{J}}_F\dot{\boldsymbol{F}}. \quad (14)$$

To construct the hybrid controller, the equation of motion (7) is substituted into eq.(13) such as

$$\boldsymbol{r}_2^{(4)} = \tilde{\boldsymbol{J}}_P\boldsymbol{M}^{-1}\left(\boldsymbol{D}\boldsymbol{\tau} - \boldsymbol{J}^T\boldsymbol{F} - \boldsymbol{K}\boldsymbol{x}\right) + \boldsymbol{J}_F\ddot{\boldsymbol{F}} + \boldsymbol{v}_1. \quad (15)$$

Approximations 5 and 6 are also considered in this equation. In eq.(15), the coefficient matrix of $\boldsymbol{\tau}$, $\tilde{\boldsymbol{J}}_P\boldsymbol{M}^{-1}\boldsymbol{D}$, is nonsingular unless the manipulator is at singular configurations. Solving eq.(15) with respect to $\boldsymbol{\tau}$, we obtain

$$\begin{aligned}\boldsymbol{\tau} &= (\tilde{\boldsymbol{J}}_P\boldsymbol{M}^{-1}\boldsymbol{D})^{-1}\{\boldsymbol{r}_2^{(4)} - \boldsymbol{J}_F\ddot{\boldsymbol{F}} \\ &\quad + \tilde{\boldsymbol{J}}_P\boldsymbol{M}^{-1}(\boldsymbol{J}^T\boldsymbol{F} + \boldsymbol{K}\boldsymbol{x}) - \boldsymbol{v}_1\}. \end{aligned} \quad (16)$$

Using this equation, dynamic hybrid position/force controller is derived as

$$\begin{aligned}\boldsymbol{\tau} &= (\tilde{\boldsymbol{J}}_P\boldsymbol{M}^{-1}\boldsymbol{D})^{-1}\{\boldsymbol{r}_{2d}^{(4)} - \boldsymbol{J}_F\ddot{\boldsymbol{F}}_d \\ &\quad + \tilde{\boldsymbol{J}}_P\boldsymbol{M}^{-1}(\boldsymbol{J}^T\boldsymbol{F} + \boldsymbol{K}\boldsymbol{x}) - \boldsymbol{v}_1\} \\ &\triangleq \boldsymbol{\tau}^*(\boldsymbol{x}, \dot{\boldsymbol{x}}), \end{aligned} \quad (17)$$

$$\boldsymbol{r}_{2d}^{(4)} = \boldsymbol{E}^{-1}\left(\begin{bmatrix} u_P \\ 0 \end{bmatrix} - 3\dot{\boldsymbol{E}}\boldsymbol{r}_2^{(3)} - 3\ddot{\boldsymbol{E}}\ddot{\boldsymbol{r}}_2 - \boldsymbol{E}^{(3)}\dot{\boldsymbol{r}}_2\right), \quad (18)$$

$$\ddot{\boldsymbol{F}}_d = \boldsymbol{E}^T\left(\begin{bmatrix} 0 \\ u_F \end{bmatrix} - \ddot{\boldsymbol{E}}^{-T}\boldsymbol{F} - 2\dot{\boldsymbol{E}}^{-T}\dot{\boldsymbol{F}}\right). \quad (19)$$

Here, u_P and u_F are new input vectors controlling the position and force, respectively, and $\boldsymbol{E}$ is the 2×2 matrix given by

$$\boldsymbol{E} = [\boldsymbol{e}_P \ \boldsymbol{e}_F]^T. \quad (20)$$

We assume that a given end point constraint can be expressed by

$$p(\boldsymbol{r}_2) = 0, \quad (21)$$

and we assume that there exists a scalar function $s(\boldsymbol{r}_2)$ and $\{p(\boldsymbol{r}_2)\ s(\boldsymbol{r}_2)\}$ are mutually independent. $\boldsymbol{e}_P$ and $\boldsymbol{e}_F$ are defined by

$$\boldsymbol{e}_F = \frac{\partial p(\boldsymbol{r}_2)}{\partial \boldsymbol{r}_2^T}, \ \boldsymbol{e}_P = \frac{\partial s(\boldsymbol{r}_2)}{\partial \boldsymbol{r}_2^T}. \quad (22)$$

Then, if the generalized coordinate of the position control direction, y_P, and the generalized force of the force control direction, f_F, are given, substituting eq.(17) into eq.(16), the closed loop becomes linear described by

$$y_P^{(4)} = u_P, \qquad \ddot{f}_F = u_F. \quad (23)$$

A variety of control laws of servo compensators are applicable. We use the following servo controller for the linearized system:

$$\begin{aligned}u_P &= y_{Pd}^{(4)} + K_{P4}(y_{Pd}^{(3)} - y_P^{(3)}) + K_{P3}(\ddot{y}_{Pd} - \ddot{y}_P) \\ &\quad + K_{P2}(\dot{y}_{Pd} - \dot{y}_P) + K_{P1}(y_{Pd} - y_P), \\ u_F &= \ddot{f}_{Fd} + K_{F2}(\dot{f}_{Fd} - \dot{f}_F) + K_{F1}(f_{Fd} - f_F). \end{aligned} \quad (24)$$

The 4th order position controller and the 2nd order force controller are used. Here, y_{Pd} and f_{Fd} are the desired values of y_P and f_F, respectively. $K_{P4}, K_{P3}, K_{P2}, K_{P1}, K_{F2}$ and K_{F1} are feedback gains.

Using the spring-mass model, hybrid position/force controller needs the desired end point trajectory to be differentiable 4 times and the desired force trajectory to be differentiable twice. This is different from the case of rigid manipulators since a hybrid controller for rigid manipulators needs the desired end point trajectory to be differentiable twice and the desired force to be differentiable 0 time.

4 Zero-Dynamics

In this section, zero-dynamics in the hybrid controller derived in the previous section are derived. First, we derive a state equation from the equation of motion. Using $[\boldsymbol{x}^T\ \dot{\boldsymbol{x}}^T]^T$ as state variables, the state equation is described as follows:

$$\begin{bmatrix} \dot{\boldsymbol{x}} \\ \ddot{\boldsymbol{x}} \end{bmatrix} = \begin{bmatrix} \dot{\boldsymbol{x}} \\ -\boldsymbol{M}^{-1}(\boldsymbol{J}^T\boldsymbol{F} + \boldsymbol{K}\boldsymbol{x}) \end{bmatrix} + \begin{bmatrix} \boldsymbol{0} \\ \boldsymbol{M}^{-1}\boldsymbol{D} \end{bmatrix} \boldsymbol{\tau}. \tag{25}$$

In the case of hybrid control, though the order of the state equation is considered to be reduced due to the constraint conditions[3], we analyze the stability conditions using eq.(25) which represents the configuration that the external force is exerted by the end effector.

We consider the transformations in the previous section as the change of coordinates and the input transformation. Eqs.(8),(9),(12) and (13) are used for this change of coordinates such as

$$\begin{bmatrix} \dot{\boldsymbol{r}}_2 \\ \ddot{\boldsymbol{r}}_2 \\ \boldsymbol{r}_2^{(3)} \\ \boldsymbol{r}_2^{(4)} \\ \dot{\boldsymbol{z}} \end{bmatrix} = \begin{bmatrix} \boldsymbol{J} & \boldsymbol{0} \\ \dot{\boldsymbol{J}} & \boldsymbol{J} \\ \tilde{\boldsymbol{J}}_P & \boldsymbol{0} \\ \dot{\tilde{\boldsymbol{J}}}_P & \tilde{\boldsymbol{J}}_P \\ \boldsymbol{T}_1 & \boldsymbol{T}_2 \end{bmatrix} \begin{bmatrix} \dot{\boldsymbol{x}} \\ \ddot{\boldsymbol{x}} \end{bmatrix} + \begin{bmatrix} \boldsymbol{0} \\ \boldsymbol{0} \\ \boldsymbol{J}_F\dot{\boldsymbol{F}} \\ \dot{\boldsymbol{J}}_F\dot{\boldsymbol{F}} + \boldsymbol{J}_F\ddot{\boldsymbol{F}} \\ \boldsymbol{0} \end{bmatrix}. \tag{26}$$

In this equation, the state variables are differentiated once. This is because the following transformations will become simple by using this equation. The new state variable $\boldsymbol{z}$ is set such that the transformation matrix in eq.(26) becomes nonsingular. $\boldsymbol{T}_1$ and $\boldsymbol{T}_2$ are the transformation matrices between $\boldsymbol{z}$ and $\boldsymbol{x}, \dot{\boldsymbol{x}}$. In our case, $\boldsymbol{x}$ is a 6 dimensional vector that consists of $\theta_1, \theta_2, \delta_1, \delta_2, \phi_1$ and ϕ_2, and $\boldsymbol{r}$ is a 2 dimensional vector. So $\boldsymbol{z}$ becomes a 4 dimensional vector. Substituting eq.(26) into eq.(25) and using eq.(17) as an input transformation, we can derive the state equation replaced by a new description

$$\begin{bmatrix} \dot{\boldsymbol{r}}_2 \\ \ddot{\boldsymbol{r}}_2 \\ \boldsymbol{r}_2^{(3)} \\ \boldsymbol{r}_2^{(4)} \end{bmatrix} = \begin{bmatrix} \boldsymbol{0} & \boldsymbol{I} & \boldsymbol{0} & \boldsymbol{0} & \boldsymbol{0} \\ \boldsymbol{0} & \boldsymbol{0} & \boldsymbol{I} & \boldsymbol{0} & \boldsymbol{0} \\ \boldsymbol{0} & \boldsymbol{0} & \boldsymbol{0} & \boldsymbol{I} & \boldsymbol{0} \\ \boldsymbol{0} & \boldsymbol{0} & \boldsymbol{0} & \boldsymbol{0} & \boldsymbol{0} \end{bmatrix} \begin{bmatrix} \boldsymbol{r}_2 \\ \dot{\boldsymbol{r}}_2 \\ \ddot{\boldsymbol{r}}_2 \\ \boldsymbol{r}_2^{(3)} \\ \boldsymbol{z} \end{bmatrix} + \begin{bmatrix} \boldsymbol{0} \\ \boldsymbol{0} \\ \boldsymbol{0} \\ \boldsymbol{r}_{2d}^{(4)} - \boldsymbol{J}_F(\ddot{\boldsymbol{F}}_d - \ddot{\boldsymbol{F}}) \end{bmatrix}. \tag{27}$$

$$\dot{\boldsymbol{z}} = \boldsymbol{T}_1\dot{\boldsymbol{x}} + \boldsymbol{T}_2\boldsymbol{M}^{-1}(\boldsymbol{D}\boldsymbol{\tau}^* - \boldsymbol{J}^T\boldsymbol{F} - \boldsymbol{K}\boldsymbol{x}). \tag{28}$$

Here, eq.(27) is a state equation of the end point $\boldsymbol{r}$. Eq.(28) is that of the new variable $\boldsymbol{z}$. $\boldsymbol{I}$ is a 2×2 unity matrix. In these new state equations, eq.(27) is linear. Eq.(27) shows that the end point position and force converge to their desired values if the position control direction and the force control direction are decoupled with respect to the constraint frame. However, eq.(28) needs to pay attention. As the state variables are differentiated once in eq.(26), eq.(28) is not changed of coordinates completely such that

$$\dot{\boldsymbol{z}} = \boldsymbol{g}(\boldsymbol{x}, \dot{\boldsymbol{x}}, \boldsymbol{u}). \tag{29}$$

Eq.(29) is changed of coordinates again as follows:

$$\dot{\boldsymbol{z}} = \boldsymbol{g}(\boldsymbol{r}_2, \dot{\boldsymbol{r}}_2, \ddot{\boldsymbol{r}}_2, \boldsymbol{r}_2^{(3)}, \boldsymbol{z}, \boldsymbol{u}). \tag{30}$$

As $\boldsymbol{z}$ is not included in eq.(27), $\boldsymbol{z}$ cannot be observed by $\boldsymbol{r}_2$, $\dot{\boldsymbol{r}}_2, \ddot{\boldsymbol{r}}_2$ and $\boldsymbol{r}_2^{(3)}$. Eq.(30) is a dynamics that is not directly controlled by a servo controller,$\boldsymbol{u}$, in which only the information of the end point position and force are used. Moreover, the stability condition depends on the stability of this dynamics. This dynamics is called zero-dynamics in hybrid control of flexible manipulators[10].

5 Simulation Results

In this section, to verify the effectiveness of the proposed control algorithm, simulation results are presented.

Parameters of the manipulator are shown in table 1. For the manipulator model, the spring-mass model are used. In the simulation of hybrid control, the environment to which the end effector is constrained have to be modeled. The environment is modeled by a spring-damper system in which the spring constant is $15000(N/m)$ and the damping coefficient is $2000(Nsec/m)$. Constraint surface is set as a plain $y = -0.3(m)$. The overview of the simulation is shown in Fig.3. The feedback gains in the servo compensators eq.(24) are set as $K_{Pt} = 5 \times 10^1$, $K_{Po} = 5 \times 10^3$, $K_{Pv} = 4 \times 10^4$, $K_{Pp} = 3 \times 10^6$, $K_{Fv} = 2 \times 10^1$ and $K_{Fp} = 8 \times 10^3$. The sampling period is set as $2msec$

Smooth trajectories are used as the desired trajectories. The desired end point trajectory is set as differentiable 9 times, in which $\dot{y}_{Pd} = \ddot{y}_{Pd} = y_{Pd}^{(3)} = y_{Pd}^{(4)} = 0$ at beginning and ending. The desired force is set as differentiable 6 times, in which $\dot{f}_{Fd} = \ddot{f}_{Fd} = 0$ at beginning and ending. These are given by

$$\begin{aligned} y_{Pd} &= 1.2 - 0.15\left\{70\left(\frac{t}{4}\right)^9 - 315\left(\frac{t}{4}\right)^8\right. \\ &+ \left. 540\left(\frac{t}{4}\right)^7 - 420\left(\frac{t}{4}\right)^6 + 126\left(\frac{t}{4}\right)^5\right\}, \end{aligned} \tag{31}$$

$$\begin{aligned} f_{Fd} &= 10\left\{-64\left(\frac{t}{4}\right)^6 + 192\left(\frac{t}{4}\right)^5 - 192\left(\frac{t}{4}\right)^4\right. \\ &\left. +64\left(\frac{t}{4}\right)^3\right\}. \end{aligned} \tag{32}$$

These trajectories are shown in Fig.4 and 5.

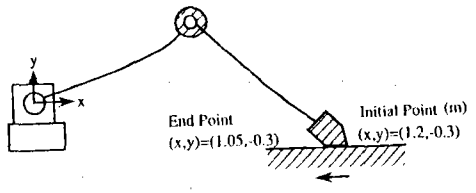

Fig.3 Simulation

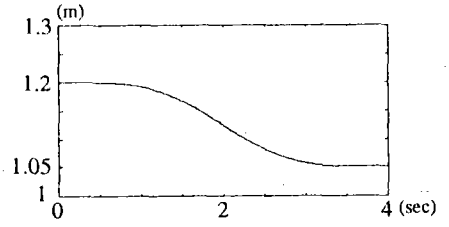

Fig.4 Desired End Point Trajectory

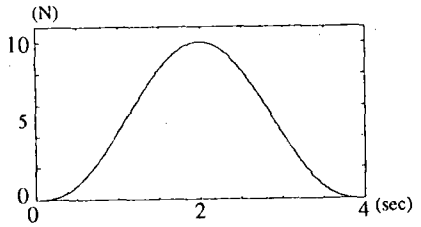

Fig.5 Desired Force

First, we analyze the stability of the zero-dynamics. We adopt the following $\boldsymbol{z}$:

$$\boldsymbol{z} = \left[\phi_1 \ \phi_2 \ \dot{\phi}_1 \ \dot{\phi}_2\right]^T. \tag{33}$$

Then, eq.(30) is regarded to be the linear time varying system such as

$$\dot{\boldsymbol{z}} = \boldsymbol{Z}_1(\boldsymbol{r}_2, \boldsymbol{F})\dot{\boldsymbol{r}}_2 + \boldsymbol{Z}_2(\boldsymbol{r}_2, \boldsymbol{F})\boldsymbol{z} + \boldsymbol{Z}_3(\boldsymbol{r}_2, \boldsymbol{F})\boldsymbol{u} + \boldsymbol{Z}_4(\boldsymbol{r}_2, \boldsymbol{F}, \dot{\boldsymbol{F}}) \tag{34}$$

The poles of eq.(34) are shown in Fig.6 when we let the manipulator precisely track the desired position and force. It can be seen from this figure that the poles exist around $\pm 200i, \pm 160i$, and eq.(34) is on the boundary of stability. This is because the damping force is considered neither in the inverse dynamic model nor in the manipulator model in the simulation.

Simulation results are shown in Fig.7-10. Fig.7 and 8 show the results of the proposed method. Fig.9 and 10

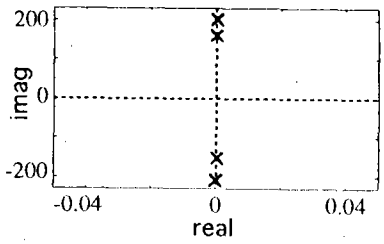

Fig.6 Stability of the Zero Dynamics

show the comparative study in which the manipulator is controlled using the hybrid control for rigid manipulators[2].

In the results of the proposed method, Fig.7 shows the end point position error, and Fig.8 shows the force error. Maximum position error is about $1 \times 10^{-4}(m)$. Maximum force error is about $0.03(N)$ These are small enough to show the effectiveness of the proposed method.

In the results of the hybrid control for rigid manipulators, Fig.9 shows the position error, and Fig.10 shows the force error. In Fig.9, the tracking error is much larger than that of the proposed method. In Fig.10, the error is as small as that of the proposed method. However, watching carefully, the error is found out to be smaller than the case of the proposed method. We consider that this is because approximations 5 and 6 are used in our proposed method. In Fig.9 and 10, a large oscillation is caused. This shows that the stability is not preserved in the hybrid control for rigid manipulators.

Table 1 Parameters of the Manipulator

	link 1	link 2
length(m)	0.724	0.725
diameter(m)	0.013	0.008
mass of end tip(kg)	4.10	1.30
bending rigidity($N \cdot m^2$)	288.8	41.4
inertia of end-tip($kg \cdot m^2$)	1.73×10^{-2}	2.22×10^{-3}

6 Conclusions

In this paper, dynamic hybrid position/force control of 2 D.O.F. flexible manipulators has been proposed. First, the flexible manipulator is modeled by using the spring-mass model. Second, a dynamic hybrid controller is constructed. In this controller, the differentiable order of the desired trajectory and the stability condition are different from the case of rigid manipulators. Lastly, to verify the effectiveness of the proposed control algorithm, simulation results are presented. The experiment is considered to be our future topic.

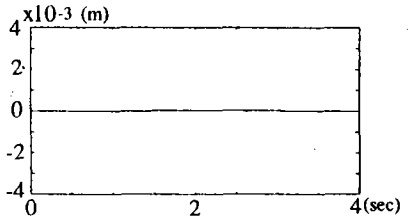

Fig.7 Position Error (Proposed Method)

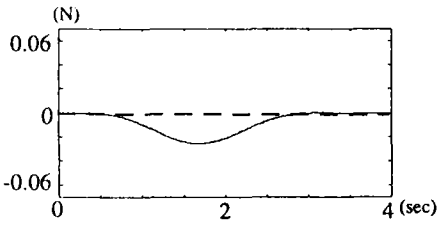

Fig.8 Force Error (Proposed Method)

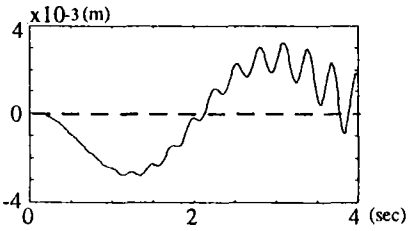

Fig.9 Position Error (Method for Rigid Manipulators)

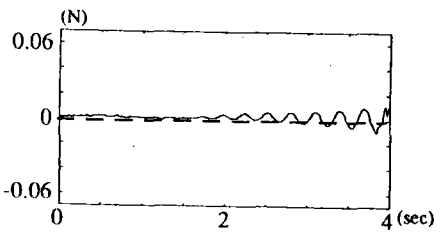

Fig.10 Force Error (Method for Rigid Manipualtors)

References

[1] M.H.Raibert,J.J.Craig. Hybrid Position/Force Control of Manipulators. *Trans. of the ASME Journal of DSMC, Vol.103, No.2, pp126-131*, 1981.

[2] T.Yoshikawa. Dynamic Hybrid Position/Force Control of Robot Manipulators—Description of Hand Constraints and Calculation of Joint Driving Force. *IEEE J. Robotics and Automation.,RA-3(5):pp386-392*, 1987.

[3] N.H.McClamroch, D.Wang. Feedback Stabilization and Tracking of Constrained Robots. *IEEE Trans. on Automatic Control, Vol.33, No.5, pp419-426*, 1988.

[4] F.Matsuno, K.Yamamoto. Dynamic Hybrid Position/Force Control of a Flexible Manipulator. *In Proc. of IEEE International Conference on Robotics and Automation pp.462-467*, 1993.

[5] M.Spong. On the Force Control Problem of Flexible Joint Manipulators. *IEEE Trans. on Automatic Control, Vol.34, No.1, pp107-111*, 1989.

[6] H.A.ElMaraghy, A.T.Massoud. Adaptive Dynamic Hybrid Position and Force Control of Flexible Joint Robot Manipulators. *In Preprint of 3rd International Symposium on Experimental Robotics pp.59-66*, 1993.

[7] K.P.Jankowski, H.A.ElMaraghy. Dynamic Decoupling for Hybrid Control of Rigid-/Flexible-Joint Robots Interacting with the Environment. *IEEE Trans. Robotics and Automation, RA-8(5), pp.519-534*, 1992.

[8] B.Siciliano, W.J.Book. A.Singular Perturbation Approach to Control of Lightweight Flexible Manipulators. *The International Journal of Robotics Research, Vol.7, No.4, pp79-90*, 1988.

[9] H.Asada, Z.-D.Ma, H.Tokumaru. Inverse Dynamics of Flexible Robot Arms: Modeling and Computation for Trajectory Control. *Trans. of the ASME Journal of DSMC, Vol.112, pp.177-185*, 1990.

[10] A.De Luca, B.Siciliano. Trajectory Control of a Nonlinear One-link Flexible Arm. *Int. J. Control, vol.50, No.5, 1699-1715*, 1989.

[11] K.Hosoda, T.Yoshikawa. Trajectory Tracking Control of 2 D.O.F. Flexible Manipulator. *Journal of the Robotics Society of Japan Vol.11, No.7, pp.1066-1072, in Japanese*, 1993.

[12] T.Yoshikawa, H.Murakami, K.Hosoda. Modeling and Control of a 3 Degree of Freedom Manipulator with 2 Flexible Links. *Proc. of IEEE Int. Conf. on Decision and Control.pp.2532-2537*, 1990.